

Transmission Computed Tomography, Tc-99m MAA Scintigraphy, and Plain Chest Radiography after Experimentally Produced Acute Pulmonary Arterial Occlusion in the Dog

Zachary D. Grossman, George Gagne, Albert Zens, F. Deaver Thomas, Charles C. Chamberlain, Amolak Singh, William N. Cohen and E. Robert Heltzman

State University of New York, Upstate Medical Center, Syracuse, New York

We have occluded segmental and subsegmental pulmonary arteries in the dog with Swan-Ganz balloon catheters or i.v. injection of autologous clot, and have studied the chest with transmission computed tomography (TCT), Tc-99m-MAA gamma imaging, and plain radiographs. The arterial occlusions were between 1 and 5 hr old at the time of imaging.

Radiographs revealed no lesions. Tc-99m MAA scans revealed ten of 11 lesions. When a TCT image was made before i.v. injection of Renografin-60, two of 11 lesions were identified; after Renografin the score was four out of ten. The appearance of lesions on TCT was highly variable.

Tc-99m-MAA gamma imaging, therefore, is far more accurate than TCT in the identification of small experimentally produced acute pulmonary arterial occlusions in the dog, and our study fails to suggest a secure place for TCT in the diagnosis of small, acute human pulmonary emboli. The commonly-held assumption that postembolic lung is oligemic is questioned.

J Nucl Med 20: 1251-1256, 1979

For many years the principal diagnostic imaging procedure for suspected pulmonary embolism has been the Tc-99m MAA lung scan. The perfusion deficits caused by embolic vascular occlusion and demonstrated by lung scanning have often been considered areas of relative oligemia. Since transmission computed tomography (TCT) effectively identifies relative oligemia based upon a gravity gradient (Fig. 1), we are exploring the value of TCT for detecting areas of supposed oligemia distal to acute pulmonary arterial occlusion. In a previous study (1) we reported the findings in five dogs with pulmonary arterial occlusions produced by Swan-Ganz balloon catheters and studied with TCT

("enhanced" and "unenhanced"), Tc-99m MAA lung scanning, and plain radiographs. In this communication we have incorporated results from additional balloon-occlusion experiments and also from experiments using i.v. injection of radiolabeled autologous clot. Moreover, the failure of chest radiography to reveal those lesions successfully identified by TCT is analyzed in terms of lesion density.

Dunnick et al. (2) reported the failure of TCT to identify three major experimentally produced pulmonary arterial occlusions; their single published TCT image, however, suffered from motion artifact and lacked a discontinuous color bar to aid in the detection of small density differences. Moreover, the reliable diagnosis of major central occlusions is not currently at issue, since Tc-99m MAA lung scanning (supplemented by Xe-133 if necessary) is almost always effective in such cases. Our study concerns small, peripheral, segmental, and sub-

Received Jan. 8, 1979, revision accepted May 23, 1979.

For reprints contact: Zachary D. Grossman, Div. of Nuclear Medicine, Dept. of Radiology, SUNY Upstate Medical Ctr., 750 E. Adams St., Syracuse, NY 13210.

segmental lesions, of the variety more likely to produce diagnostic problems at the clinical level.

Since lung perfusion distal to a pulmonary arterial occlusion is different from that of normal lung, we reasoned that TCT image "enhancement" by peripheral i.v. injection of contrast medium might well increase any density difference between normal and postocclusive areas. Our original supposition was that the contrast medium would increase the density of normal lung more than it would the density of postocclusive lung. On the other hand, postembolic lung may still be perfused by the bronchial circulation in the normal dog, and thus contrast medium might reach the postembolic area in sufficient concentration to prevent the development of such a density difference.

The most prominent lesion detected by TCT was analyzed in order to establish whether sufficient radiographic contrast was present for detection on conventional radiography.

MATERIALS AND METHODS

Vascular blockade. In anesthetized mongrel dogs weighing between 20 and 30 kg pulmonary arteries were occluded by two methods (a) Swan-Ganz balloon catheters, and (b) i.v. injection of preformed radiolabeled autologous clot.

Swan-Ganz balloon catheters. Segmental or subsegmental pulmonary arterial branches were occluded with 5-French or 7-French Swan-Ganz balloon catheters as described previously (1).

Embolus occlusion. Glass microspheres, mercury droplets, gelfoam particles, and other similar substances were excluded, since such material would alter lung density and produce spurious TCT findings. We chose to form and then inject radioactive thrombi into the femoral vein, thus closely mimicking the natural events of peripheral venous-to-lung embolization in humans. The thrombus formation and injection proceeded as follows. Three hours before anesthesia, 5 cc of peripheral venous blood were drawn into a syringe containing 100 μ Ci of Tc-99m MAA, and the blood and tracer were thoroughly mixed. In pilot studies, siliconized tapered-end plastic tubes of various lengths (5-15 cm) and internal diameters (3-8 mm) were rinsed with thrombin solution (1000 NIH units/ml), filled with the tracer-blood mixture, and set aside for 3 hr, and solid radioactive clots were formed. Under anesthesia, the dog's femoral vein was punctured by the Seldinger technique and dilated until it accepted an angiographic sheath selected to fit the small end of the clot-containing tube. The dog was then placed under the gamma camera, the end of the tapered tube inserted into the i.v. sheath, and the clot forced into the vein by saline injection through the tube. The camera followed the progress of the clot into the pulmonary bed, detecting any fragmentation

that might occur. A wide variety of clot sizes can thus be introduced and located.

Use of radioactive thrombi does not exclude subsequent lung scanning with Tc-99m MAA particles. Thus, scintiphotos revealing increased areas of radioactivity were followed by scintiphotos revealing "perfusion deficits," establishing that the thrombi injected did indeed occlude the distal pulmonary circulation (Fig. 2). For production of lesions, we selected clots formed in a siliconized plastic tube 5 cm long and 8 mm wide; these were injected through a sheath 8 mm in diameter.

Instrumentation. The gamma camera* used an all-purpose collimator. The TCT unit† (18-sec scanning time) provided an 8-mm slice thickness with a 42-cm scan diameter. TCT images were viewed and photographed from both black-and-white and color monitors (3). Respiratory artifact was almost eliminated by hyperventilating the anesthetized animal between scans. For "enhanced" TCT, 100 cc Renografin-60‡ were injected into a limb vein.

Film and radiographic technique. Chest radiographs were produced at 60 kVp (HVL about 2 mm of aluminum) with a conventional diagnostic x-ray unit using Dupont 2DC film and Dupont Hi Plus screens. The film was rapid-processed at manufacturer's specifications and viewed under conventional conditions.

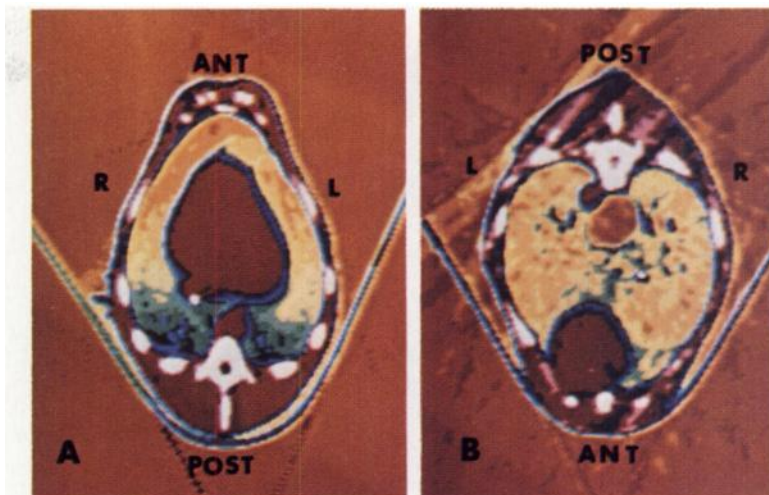
Imaging sequence. The fluoroscopic, radiographic, computed tomographic, and radionuclide studies were obtained in the following sequence in different portions of the investigation.

(a) Balloon occlusion: Fluoroscopic positioning of at least one Swan-Ganz catheter, baseline radiographs with balloon(s) *deflated*, baseline TCT with balloons *deflated* (prone and supine), unenhanced TCT with balloons *inflated* (prone and supine), contrast-enhanced TCT with balloons *inflated* (prone and supine), final radiographs, and Tc-99m MAA lung scan. (Baseline TCT was omitted after the first three animals.)

(b) Embolic occlusion: Baseline radiographs, injection of preformed thrombus and chest scintigrams, injection of Tc-99m-MAA particles and chest scintigram, "unenhanced" TCT (prone and supine), "enhanced" TCT (prone and supine), and final radiographs.

Analysis of expected radiographic sensitivity. Radiographic contrast was calculated using the relationship $C = 0.4343 \gamma(\mu_1 - \mu_2) x$, where C = radiographic contrast, γ = gamma of the film-screen system, μ_1 and μ_2 = linear attenuation coefficients of the lesion and lung, respectively, and x = thickness (4). Contrast (C) here refers to the radiographic contrast produced by the lesion in question compared with a similar thickness of adjacent normal lung. The gamma (γ) for our film-screen system was found to be 2.8. The lesion thickness from front to back was determined directly from the TCT images. The linear attenuation coefficients (μ_1, μ_2) were obtained by assuming an effective beam energy of

FIG. 1. Supine transaxial image (A) of lower thorax of anesthetized dog reveals striking anterior-to-posterior increasing density gradient. Discontinuous color bar is arranged so that progressively greater densities are toward *top*. Note predominance of blues and greens in dependent portions of both lungs, and predominance of yellows and oranges more ventrally. Prone transaxial image (B) of anesthetized dog reveals loss of most of gradient. Lung density is largely uniform from front to back.



30 keV and an effective atomic number 7.4 (as in water) for the lesion and normal lung tissue (5). Lesion mass density, estimated from TCT attenuation data and a lung density of 0.3 g/cm^3 , was found to be $\sim 0.37 \text{ g/cm}^3$. The mass attenuation coefficient for water at 30 keV then gave μ_1 and $\mu_2 = 0.13 \text{ cm}^{-1}$ and 0.10 cm^{-1} , respectively (6). The difference in attenuation produced by the lesion, compared with the adjacent normal lung, was applied to the H & D curve for the film-screen combination used, in order to estimate the difference in film density produced.

RESULTS

To date, pulmonary arterial occlusions have been

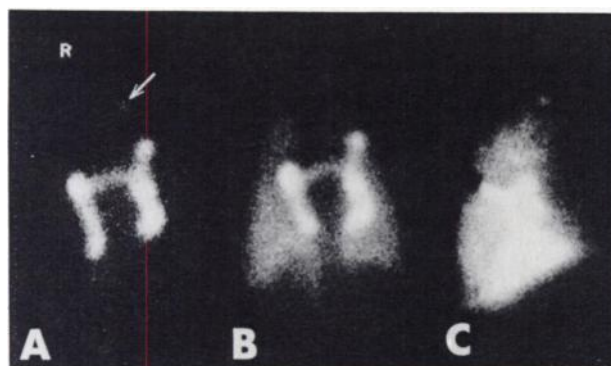


FIG. 2. Posterior scintigram (A) of thorax after i.v. injection of Tc-99m MAA labeled autologous clot, 15 cm long, reveals that thrombus has lodged in branches of right and left pulmonary arterial tree, with connecting bridge across main pulmonary artery segment. Solitary fragment on left (arrow) has separated from main thrombus and progressed distally. Posterior scintigram (B) of dog thorax 5 min after i.v. injection of 1 mCi of Tc-99m MAA particles reveals perfusion deficits in left apex and the right base, probably involving apical-posterior segment of left upper lobe and posterior-basal segment of right lower lobe. Lateral view of thorax (C) immediately after (B) again reveals posterior-basal perfusion deficit. However, additional subsegmental perfusion deficit in posterior segment of right upper lobe is now identified. (Apex is poorly visualized on lateral view because of overlying scapula.)

produced in nine dogs, seven with one vessel occluded and two with two, making a total of 11 occlusions. Eight were produced by Swan-Ganz catheters and three by Tc-99m MAA-labeled emboli (one in the left lower lobe and two in the right lower lobe).

Table 1 lists the types of occlusion and the findings (consensus of four observers) for TCT with (“enhanced”) and without (“unenhanced”) contrast medium, and for Tc-99m MAA gamma scintigraphy. All emboli and seven of the eight balloon occlusions were studied by both enhanced and unenhanced TCT.

Unenhanced TCT identified only two of 11 lesions, both balloon occlusions, which appeared as foci of increased density. Enhanced TCT revealed three additional balloon-produced lesions as areas of at least 100 Hounsfield units (H.U.) *greater* density than surrounding or contralateral normal lung (Figs. 3 and 4). The effect of intravenous contrast medium was not consistent, however, since (a) no embolus was localized, and (b) two other balloon-produced lesions were partially “brought out” by contrast medium as foci of slightly *decreased* density; these areas “enhanced” less than normal lung, but the density difference was insufficient for prospective diagnosis (Fig. 5).

No reliable correlation between the duration of occlusion and TCT findings was apparent. The two balloon-produced lesions revealed without contrast medium were 4 hr and 2.67 hr old. Both older and younger balloon-produced lesions were not identified. Similarly, positioning was not a consistent factor in lesion identification; some lesions were better demonstrated prone and others supine.

Tc-99m MAA lung scans failed to reveal only one lesion—a radiolabeled embolus.

Uniformly, chest radiographs before and after TCT were unremarkable. The very low calculated radiographic contrast (C) was found to be 0.072 for the most prominent lesion on TCT (200 Hounsfield units density increase). The density difference on the processed film



FIG. 3. Supine transaxial image (enhanced) of anesthetized dog (lesion 1) reveals region of increased density at left base (arrows). Lesion was balloon-produced and was not demonstrated by unenhanced TCT after an hour of balloon inflation. Twenty min after peripheral i.v. injection of 100 cc Renografin 60, however, area of increased density was observed. Lesion is approximately 125 Hounsfield units denser than surrounding or contralateral lung. Reproduced with permission of Gross ZD, et al (1).



FIG. 4. Prone transaxial image of anesthetized dog (lesion 3) reveals increased density at left base (arrows). Lesion was demonstrated only by enhanced TCT and was approximately 200 Hounsfield units denser than surrounding or contralateral normal lung. Reproduced with permission of Gross ZD, et al (1).

between the region of the lesion and the immediately adjacent area, as calculated from the H & D curve, was ~ 0.05 optical density units.

DISCUSSION

The increased density of two balloon-produced occlusions on unenhanced TCT is not surprising, in view of the well-known changes on chest radiography that occasionally follow embolization. The relatively lower-than-normal density, detected in two balloon-produced lesions by enhanced (but not unenhanced) TCT, is also

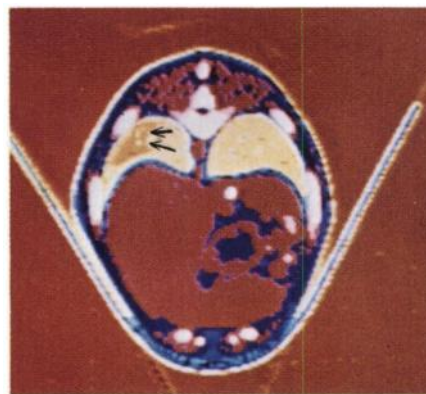


FIG. 5. Prone transaxial image of lesion No. 1 reveals area of slightly decreased density at left base (arrows). Density difference between normal and abnormal lung varied between 50 and 95 Hounsfield units. Such small density differential is easily obscured by minimal artifact or errors in positioning, and this lesion was not identified without foreknowledge of catheter placement.

not surprising. The intravenous infusion of contrast medium would be expected to produce a generalized slight increase in overall body radiographic opacity. Since flow distal to a pulmonary arterial occlusion is assuredly much slower than in normal lung, postocclusive regions might well be expected to "enhance" to a lesser degree than surrounding or contralateral normal lung. However, the discrepancy between postocclusive and normal lung thus revealed would be minor. Indeed, such lesions were never more than 95 Hounsfield units less dense than normal lung, and the lesions showed too poorly for reliable prospective diagnosis.

The most unanticipated finding in this study was the increase in density of three balloon-produced lesions, only after injection of contrast medium. None of these lesions was seen on unenhanced TCT. Tissue injury and interstitial collection of contrast medium, too subtle to be observed on conventional radiographs, is one possible cause. Other causes of postocclusive density increase—e.g., partial alveolar collapse, accumulation of minimal intra-alveolar fluid, etc.—also should have produced increased density on "unenhanced" studies.

The failure of chest radiography in all cases reflects the superior contrast resolution of TCT. The most prominent lesion (Fig. 4) was 200 Hounsfield units denser than contralateral or surrounding normal lung. Although sufficiently large for spatial resolution on plain radiographs, the difference in attenuation between the lesion and normal adjacent lung was insufficient to produce detectable radiographic contrast. The calculated optical density difference was almost at the threshold of visual detectability under ideal viewing conditions. Despite the use of a radiographic grid, some scatter persisted; this scatter, together with superimposition of other structures, further contributed to decreased radiographic detectability. Thus, the inability of conventional radiographs to reveal the lesion conformed to theoretical ex-

TABLE 1

| Occlusion | Type and location of balloon occlusions | Lung density change on TCT without contrast medium (unenhanced) | Lung density change on TCT with contrast medium (enhanced) | Comment on TCT studies | Duration of occlusion at time of TCT (hrs) | | Perfusion on Tc-99m-MAA lung scan |
|--|---|---|--|---|--|------------|-----------------------------------|
| | | | | | "Unenhanced" | "Enhanced" | |
| 1 | L.L. lobe, segmental | None | ↑100–125 H.U.* | TCT supine only | 1 | 1.3 | Deficit |
| 2 | L.L. lobe, segmental | None | ↑100–125 H.U. | Lesion better identified prone | 1 | 1.3 | Deficit |
| 3 | L.L. lobe, segmental | None | ↑200 H.U. | Lesion better identified prone | 1 | 1.3 | Deficit |
| 4 | L.L. lobe, segmental | ↑100–125 H.U. | | No contrast study performed | 4 | | Deficit |
| 5 | L.L. lobe, segmental | ↑150 H.U. | ↑150 H.U. | Lesion identified only supine, better seen "unenhanced" | 2.1 | 3.1 | Deficit |
| 6 | L.L. lobe, segmental | None | ↓50–95 H.U. | Lesions identified only with foreknowledge of balloon placement | 4 | 4.5 | Deficit |
| 7 | L.L. lobe, segmental | None | ↓50–95 H.U. | | 3.5 | 4.5 | Deficit |
| 8 | R.L. lobe, subsegmental | None | None | | 2.3 | 3.5 | Deficit |
| <u>Type and Location of Embolic Occlusions</u> | | | | | | | |
| 9 | R.L. lobe, subsegmental | None | None | | 2.3 | 3 | Normal |
| 10 | L.L. lobe, segmental | None | None | | 1.3 | 2 | Deficit |
| 11 | R.L. lobe, segmental | None | None | | 1.3 | 2 | Deficit |

* H.U. denotes Hounsfield units.

pectations.

The failure of unenhanced TCT to demonstrate nine of 11 lesions strongly questions the assumption that postembolic lung is oligemic. The bronchial collateral circulation may remain patent after an acute pulmonary arterial occlusion, and the degree to which bronchial circulation supplies the lung distal to a pulmonary arterial occlusion determines postocclusion blood flow. Moreover, regardless of bronchial collateral flow, the true blood mass in a given volume of postembolus lung might not be reduced, since stagnant or slow-moving blood in the vascular bed distal to an occlusion does not constitute true oligemia. Taplin et al. (7) and Nichols et al. (8) have successfully identified emboli by labeling the red cell pool distal to emboli with inhaled ¹⁵O-labeled

carbon dioxide. The high detection rate of the ¹⁵O-carbon dioxide method supports the contention that distal to most emboli the pulmonary vascular tree remains filled with static or slow-moving blood. The visual impact of a pulmonary angiogram and a Tc-99m MAA scan often results in an unwarranted assumption that distal to emboli, when the chest radiograph is normal—i.e., when infarction is not suspect—the lung has "less blood." Perfusion deficits thus revealed, however, are likely just as "bloody" on a "blood-mass-per unit-volume" basis as normal lung.

CONCLUSIONS

1. In our series of 11 occlusions, oligemia was not

identified in postocclusive lung. Perhaps a larger series would have revealed occasional oligemia, corresponding to the clinically observed "sign of Westermark." Moreover, study of larger lesions and of occlusions more than 5 hr old might well reveal evolving density changes not observed in the acute experiments described here.

2. TCT is far less accurate than Tc-99m MAA lung scanning in the diagnosis of acute experimental pulmonary arterial occlusion in the dog.

3. The variability of TCT findings in this condition is great, and includes increased lung density (unenhanced), increased lung density (when enhanced only), and slight relative decrease in lung density (when enhanced). To some extent, these findings parallel those of clinical radiography, in that the findings produced by human pulmonary emboli are protean. Nonetheless, the observation of increased density after contrast infusion was unexpected, and its cause remains obscure.

4. Lesion density analysis confirms that many of the subtle postocclusion changes detected by TCT would not be identified by conventional radiographs.

5. This study fails to indicate a secure place for TCT, at the present state of the art, in the diagnosis of pulmonary embolism.

FOOTNOTES

- * Ohio Nuclear Series 100,
- † Ohio Nuclear Delta Scan 50,
- ‡ Squibb, New Brunswick, NJ.

REFERENCES

1. GROSSMAN ZD, THOMAS FD, GAGNE G, et al: Transmission computed tomographic diagnosis of experimentally-produced acute pulmonary vascular occlusion in the dog. *Radiology* 131: 767-769, 1979
2. DUNNICK NR, DOPPMAN JL, PEVSNER PH: Failure of computer assisted tomography to detect experimental acute obstruction of major pulmonary arteries. *J Comput Assist Tomogr* 1: 330-382, 1977
3. RICHARDSON RL: An inexpensive color display for computed tomography scanners and other imaging systems. *J Comput Assist Tomogr* 2: 375-377, 1978
4. MEREDITH WJ, MASSEY JB: *Fundamentals of Physics and Radiology*, 3rd edition. Chicago, Year Book Medical Publishers, Inc, 1977, pp 233-237
5. TER-POGOSSIAN MM: *The Physical Aspects of Diagnostic Radiology*. New York, Hoeber Medical Division, Harper & Row, 1967, p 161
6. JOHNS HE, CUNNINGHAM JR: *The Physics of Radiology*. 3rd edition. Springfield, IL, Charles C Thomas, 1969, p 746
7. TAPLIN GV, CHOPRA SK, MACDONALD NS, et al: Imaging small pulmonary ischemic lesions after radioactive carbon monoxide inhalation. *J Nucl Med* 17: 866-871, 1976
8. NICHOLS AB, COHAVI S, HALES CA, et al: Scintigraphic detection of pulmonary emboli by serial positron imaging of inhaled 150-labeled carbon dioxide. *N Engl J Med* 299: 279-284, 1978

**CENTRAL CHAPTER SPRING MEETING
SOCIETY OF NUCLEAR MEDICINE**

March 27-29, 1980

St. Paul Radisson Hotel

St. Paul, Minnesota

The Spring Meeting of the Central Chapter of the Society of Nuclear Medicine will be held March 27-29, 1980 at the St. Paul Radisson Hotel in St. Paul, Minnesota.

The theme of the meeting is "An Update and What's New in Nuclear Medicine, with Emphasis on Emission Tomography." The meeting will be conjoint with physicians, physicists, and technologists. Commercial exhibits will also be displayed.

For information contact:

Deborah A. Churan, Executive Director
Central Chapter, Society of Nuclear Medicine
P.O. Box 160
Crystal Lake, IL 60014

Papers on all subjects are welcome. Submit abstracts to:

Marion E. Goldberg, MD
University of Minnesota Hospitals
Minneapolis, MN 55455

**DEADLINE FOR RECEIPT OF ABSTRACTS:
FEBRUARY 1, 1980**